The effect of surface dust availability on the timing of Martian dust storms.

Christopher Lee[1], Mark Richardson[2], and Claire Newman[2]

[1]University of Toronto
[2]Aeolis Research

November 24, 2022

Abstract

Current state-of-the-art models of dust lifting in Mars climate models track finite surface-dust reservoirs but use a constant lifting coefficient at all locations until the reservoir is exhausted (e.g. Newman and Richardson, 2015). In this work, the MarsWRF General Circulation Model (GCM) is modified to adjust the dust lifting coefficient as a function of a dust availability parameter that varies with location. A "Dust Cover Index" derived from remote albedo observations is used to limit the availability of dust on the surface, without limiting the total mass of dust in the reservoir. Simulations with a two moment scheme (Lee et al., 2018) are compared with a nominal case where the unlimited dust is equally available across the planet. Idealized simulations are then used to show that the spatial location of dust availability controls the timing of large dust storms during the annual storm season, and this relationship may be inverted to provide a weak constraint on the lifting locations that lead to observed dust storms on Mars.

The effect of surface dust availability on the timing of Martian dust storms

Christopher Lee[1,2] & Mark I. Richardon[2] & Claire E. Newman[2]

(1) University and Toronto, (2) Aeolis Research

Contact Information:
Christopher Lee
Email: clee@atmosp.phyiscs.utoronto.ca

UNIVERSITY OF TORONTO

AEOLIS RESEARCH

Introduction

MarsWRF [3] currently lifts dust with constant efficiency across the planet regardless of the surface composition, terrain, or dust abundance. Where finite dust is included in simulations[2] the dust lifting maintains the same efficiency until the reservoir is exhausted.

In this study we include a static, spatially varying dust availability map based on the Dust Cover Index derived from TES observations [4]. This dust availability map, as well as idealized maps are used to show that a spatial variation in lifting efficiency can affect the timing of the seasonal dust storms. In some cases, the lack of available dust in particular locations also leads to new behaviour in later seasons.

The static availability map controls the dust lifting in a similar way to an equilibrated finite dust simulation but allows the possibility of increasing the lifting difficulty as the surface dust is removed prior to exhaustion, preventing the complete exhaustion of some dusty regions.

TES Dust Cover Index

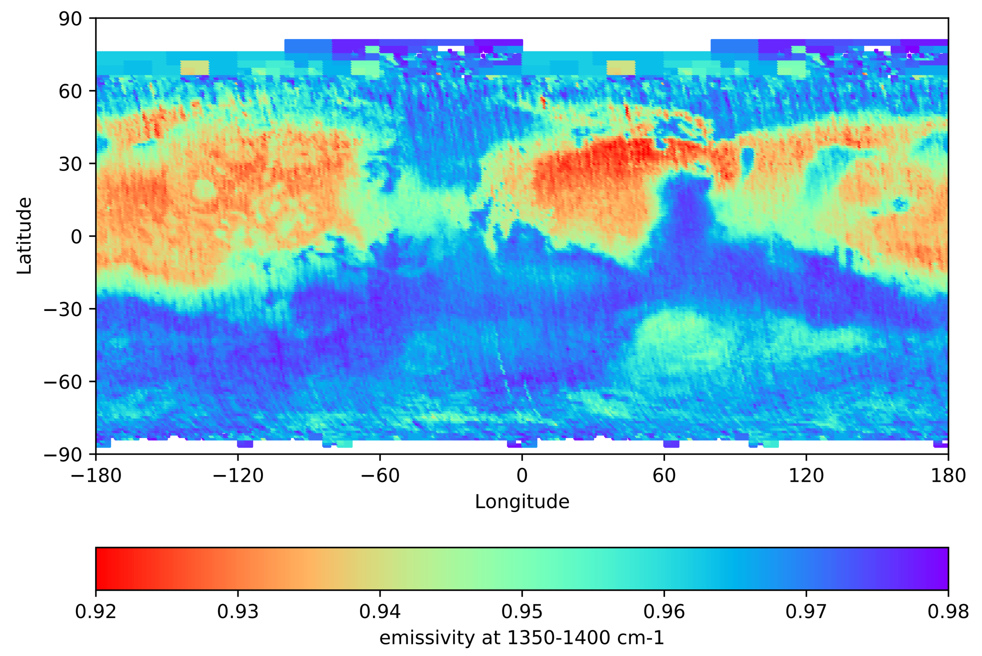

Figure 1: The surface emissivity in an infra-red band measured by the Thermal Emission Spectrometer (TES) [4]. This emissivity is assumed to map to a dust areal coverage and therefore to average dust availability.

For this study, we use the TES DCI map (figure 1) and map the observed surface emissivity E to an arbitrary measure of availability $A = S \cdot E + A_0$. Where the scale factor S and offset A_0 are used to provide a value between 0 and 1. This availability is used to scale the lifting efficiency at each point in the simulation.

In typical usage, this equation might map emissivity of 0.92 to maximum dust availability and 0.98 to a minimum dust availability, assuming dust is brighter than bedrock. In all cases where surface ice overlays the dust, no lifting is allowed regardless of the efficiency. We also assume the dust abundance to be effectively infinite and that lifted dust does not alter the areal coverage of the remaining dust.

We run MarsWRF with the two-moment dust and water ice model [1] with identical conditions in each simulation except for the dust availability map. The simulations are listed in table 1 and include a control, two simulations with DCI derived maps, and five idealized maps with hemispheric lifting. The idealized simulations are unrealistic and unstable over multiple years but highlight the effect of different lifting regions.

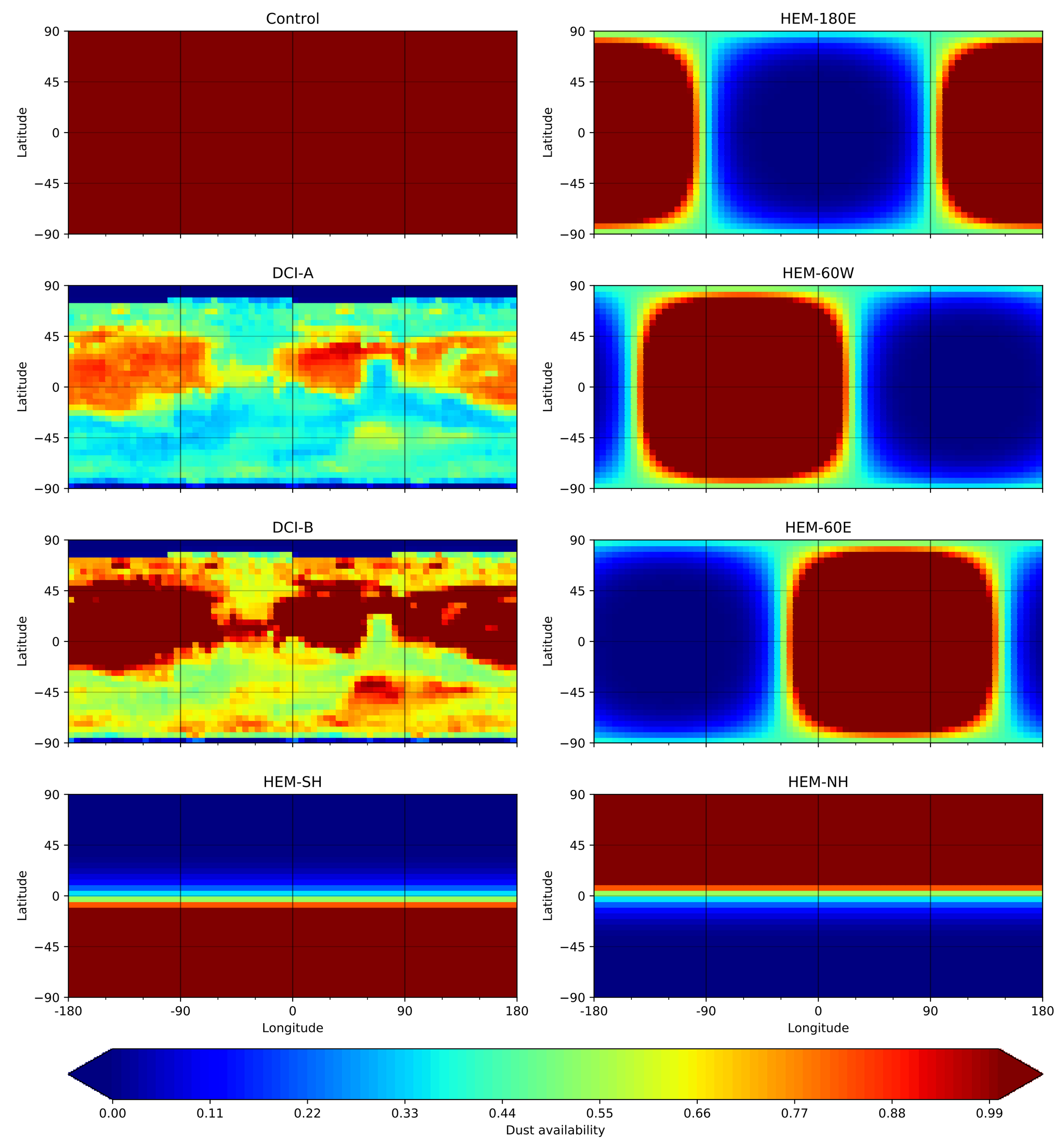

Figure 2: Dust availability maps referenced in the text and in table 1.

Label	Simulation
control	Two moment scheme uniform dust availability [1]
DCI-A	Dust availability controlled by DCI maps scaled from [0.92,0.98] to [1,0]
DCI-B	as DCI-A scaling [0.95,0.98] to [1,0]
HEM-SH	Hemispherically constant DCI centered on the south pole
HEM-NH	Hemispherically constant DCI centered on the north pole
HEM-180E	centered on the equator at 180 longitude
HEM-60W	centered on the equator at 60 west longitude
HEM-60E	centered on the equator at 60 east longitude

Table 1: Simulations using different DCI maps and conditions. The control simulation reproduces a constant lifting efficiency model. The DCI simulations use the TES DCI map. The HEM simulations include a constant unity efficiency over one hemisphere, and constant zero efficiency over the other with a short transition between the two.

References

[1] C. Lee, M.I. Richardson, C.E. Newman, and M.A. Mischna. *Icarus*, 311, 2018.

[2] Claire E. Newman and Mark I. Richardson. *Icarus*, 257:47–87, September 2015.

[3] M. I. Richardson, A. D. Toigo, and C. E. Newman. *Journal of Geophysical Research*, 112(E9):1–29, September 2007.

[4] S. W. Ruff and P. R. Christensen. *Journal of Geophysical Research: Planets*, 107(E12):2–1–2–22, December 2002.

Results and Analysis

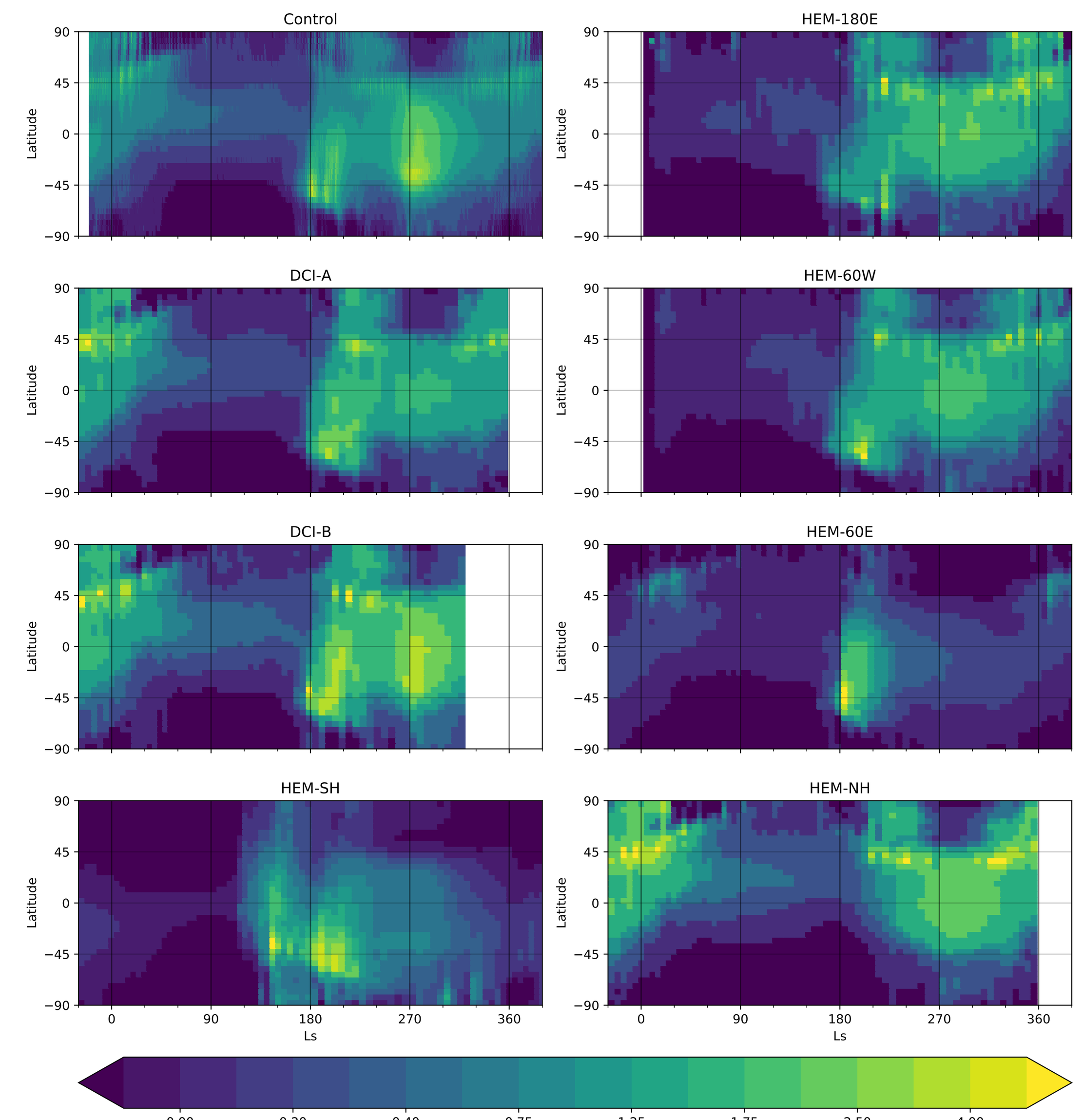

Figure 3: Dust opacity as a function of latitude and time. Simulations were started from the end of the control simulation and run for one at least one additional year. White space indicates missing data but not model problems.

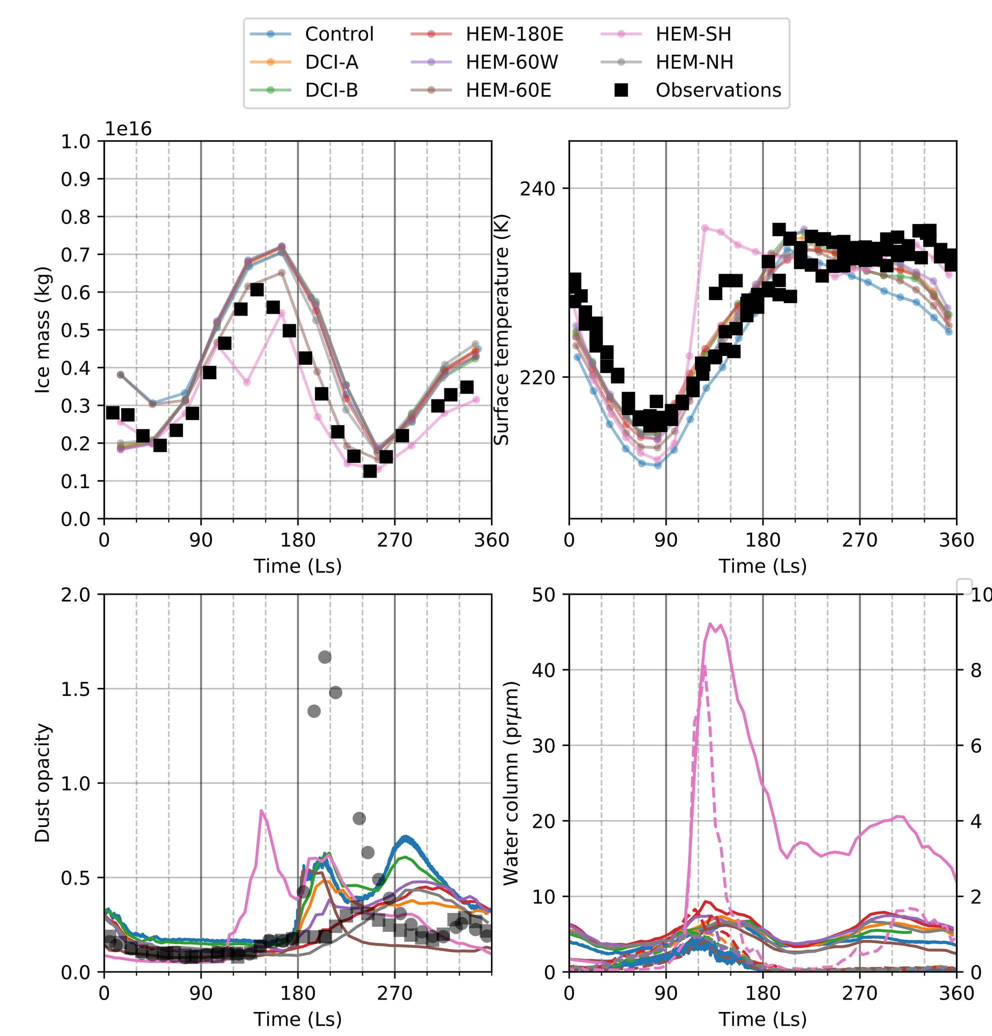

Figure 4: (top left) Global carbon dioxide ice mass. (top right) Tropical 15 micron brightness temperature. (bottom left) Tropical water vapour (solid) and ice (dashed) abundance. (bottom right) Tropical visible dust optical depth 15 micron effect temperature for various simulations.

Seven simulations reproduce the dust storm starting at around Ls=200, and several simulations produce the Ls=270 storm. The location of dust availability suggests that the Ls=200 starts near Hellas as the cap edge recedes, and the Ls=270 storm starts in Tharsis. The TES-DCI maps reduce the effect of this second storm by decreasing the efficiency over those regions.

Only the HEM-SH simulation produces an early (unrealistic) aphelion storm, caused in part by the *lack* of dust in the northern hemisphere during early summer that changes the flux of water into the atmosphere. This migrating water then triggers the storm during the aphelion cloud season. However, since the water ice albedo is a tunable representation of the true surface composition, this effect could be reduced by increasing the albedo of the northern polar ice.

The remaining HEM simulations produce similar storms with varying magnitudes and lifetimes. The maps with Hellas-region lifting reproduce the TES observed Ls=200 storm better than without lifting at these longitudes. Any simulations with some NH lifting produces northern spring cap edge storms that dampen the water cycle in early summer.

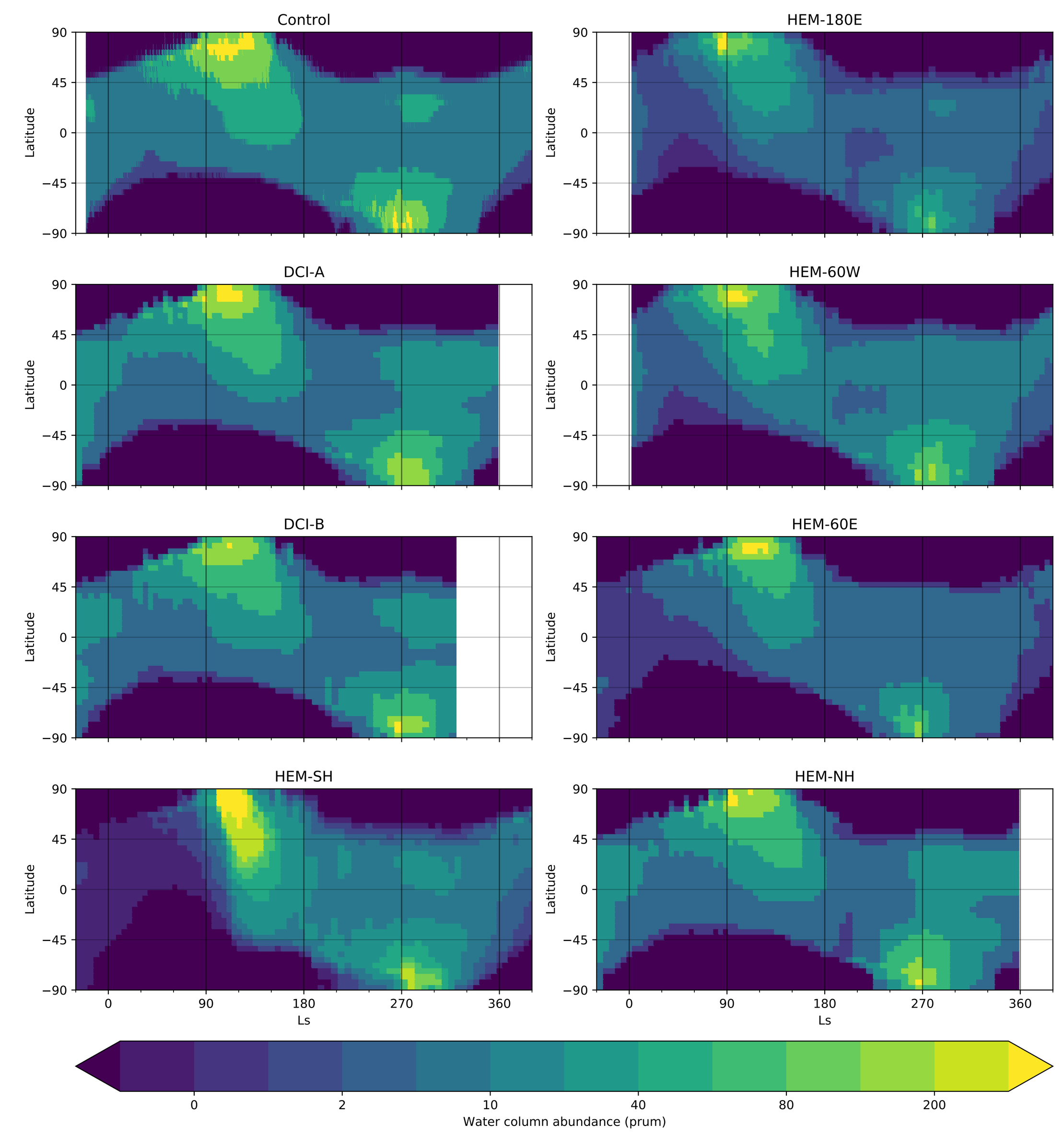

Figure 5: Water vapour column abundance for the same simulations as in figure 3.

Summary

- Dust availability (or coverage) maps can control the timing and location of the large dust storms found in [1].
- The dust availability only provides a relative measure of dust coverage based on emissivity.
- Lifting over Hellas is needed for the Ls=200 storms, and lifting over Tharsis for the Ls=270 storms.
- With a suitable mapping from surface dust mass to coverage, this could delay the total depletion of dust reservoirs on the surface.